ORIGINAL PAPER

Environmental Impact Assessment of Liquid Waste Ponds in Uranium Milling Installations

C. P. Naveira-Cotta · E. M. Pontedeiro · R. M. Cotta · J. Su · M. T. van Genuchten

Abstract A detailed environmental impact assessment is required in many countries when considering the disposal of wastes containing radioactive materials. In this paper we present hybrid numerical-analytical solutions for the subsurface transport of radioactive contaminant decay chains that may be used for such an assessment. The model involves the advective–dispersive transport of multiple radionuclide species within separate but coupled saturated and unsaturated soil domains. The resulting partial differential equations were solved using the Generalized Integral Transform Technique to yield analytical expressions for the concentration distributions versus distance, and analytical or numerical solutions as a function of time. The potential of the hybrid modeling approach is illustrated by means of an environmental impact assessment of an uranium milling liquid waste pond near Caetité, Brazil. Calculated radionuclide concentration distributions were for this purpose used in subsequent radiation dose calculations. Several scenarios were analyzed, including operational, human intrusion, farmer/road builder, and leaching scenarios. Numerical results show that for all scenarios analyzed the total dose is less than the Brazilian regulatory dose limit of 0.3 mSv/year above natural background for a period of 10,000 years.

List of symbols
C_i Concentration of i-th radionuclide in decay chain [Bq/m^3]
C^* Filtered concentrations [Bq/m^3]
D Dispersion coefficient [m^2/year]
f_i Concentration of the i-th radionuclide at the inlet [Bq/m^3]
h Mass transfer coefficient [1/year]
i Subscript, refers to the i-th radionuclide in the decay chain
Kd Distribution coefficient [m^3/kg]
L Length of the transport domain [m]
N_r Total of species in the radionuclide decay chain
q Recharge rate given by the Darcy-Buckingham equation [m/year]
R_i Retardation factor of i-th radionuclide [-]
t Time [year]
V Pore-water velocity [m/year]
x Distance [m]

Greek letters
α Dispersivity [m]
λ Eigenvalue
θ Variable water content in the unsaturated zone [m^3/m^3]
μ Decay rate [1/year]
μ_i Decay rate of the i-th radionuclide [1/year]
φ Eigenfunction

C. P. Naveira-Cotta · R. M. Cotta (✉) · M. T. van Genuchten
Mechanical Engineering Department, Center for Analysis and Simulations in Environmental Engineering, CASEE, POLI&COPPE, Universidade Federal do Rio de Janeiro, Cidade Universitária, Cx. Postal 68503, Rio de Janeiro, RJ 21945-970, Brazil
e-mail: cotta@mecanica.coppe.ufrj.br

E. M. Pontedeiro · J. Su
Nuclear Engineering Department, POLI&COPPE, Universidade Federal do Rio de Janeiro, Cidade Universitária, Cx. Postal 68503, Rio de Janeiro, RJ 21945-970, Brazil

Introduction

Regulatory bodies in many countries require a detailed environmental impact assessment when considering the disposal of solid and liquid wastes from industrial activities involving radioactive materials [1–3]. The assessment typically includes an analysis of the transport of radionuclide decay chains through engineered and natural barriers into underlying and downgradient soil and aquifer systems, for both design and operation licensing purposes. Industrial activities producing radioactive materials include nuclear power production, electricity generation, petroleum and natural gas production, and mining and milling operations [4–6]. Part of the environmental impact assessment generally pertains to the long-term effects to human health [7, 8] of radionuclides in the geosphere through all possible pathways (soil, water, air). In order to simulate the transport of radionuclide decay chains in soils, one must solve the coupled system of transport equations for each species in the chain for the hydrologic and geochemical conditions of the specific site being considered.

Several powerful and well-tested analytical and numerical simulation tools are publicly or commercially available for the required calculations. While many field problems may require comprehensive one- or multi-dimensional numerical models simulating transient water, heat and/or contaminant transport [9, 10], some transport problems are better addressed using simplified analytical or quasi-analytical models. As pointed out in many studies (e.g., [11–15]), analytical models are useful for initial or approximate analyses of alternative pollution scenarios, conducting sensitivity analyses to investigate the effects of various parameters or processes on transport, extrapolating results over large times and spatial scales where numerical solutions become impractical, serving as screening models, providing benchmark solutions for more complex transport processes that cannot be solved analytically, and for testing more comprehensive numerical solutions of the governing transport equations.

Especially attractive for long-term environmental impact assessments are classical integral transform methods, which during the past several decades have slowly evolved into very flexible hybrid numerical-analytical approaches that offer user-controlled accuracy and more efficient computational performance for a wide variety of a priori non-transformable problems [16, 17], including nonlinear mass transfer and heat and fluid flow applications related to environmental modeling [18]. The hybrid method in various forms has been applied over the years to a large number of environmental problems [18–24]. The approach is particularly well suited for benchmarking purposes because of its automatic error control features, and by retaining the same characteristics as a purely analytical solution. In addition to error control and estimation, an attractive aspect of the method is its straightforward extension to multi-dimensional situations with only a moderate increase in computational effort as compared to one-dimensional applications [25]. This is due to the hybrid nature of the solution process since the analytical part is employed for all but one independent variable, while the numerical part is used only for integration of a system of ordinary differential equations (ODE) in one single independent variable, usually the time variable.

In this study we used the Generalized Integral Transform Technique (GITT) in a hybrid numerical-analytical solution of the set of advection–dispersion equations describing the migration of radioactive decay chains in finite porous media, as implemented within the *Mathematica* 5.2 platform [26]. The one-dimensional transient formulation is applicable to chains of any prescribed length and for varying retardation (sorption) and decay properties among the radionuclides involved. The method can be implemented using either prescribed initial concentrations within the repository as part of the transport domain, or by invoking inlet concentrations obtained from solutions of the Bateman equations [27] assuming a well-mixed repository releasing its radionuclides over time [28, 29]. First- or third-type boundary conditions can be used for the leaching (inlet) boundary, and second- or third-type conditions for the downgradient (outlet) side of the transport domain. A simple filtering strategy can further be employed to homogenize the leaching boundary condition, whereas the NDSolve routine [26] is used to numerically solve the transformed ODE system. Each transformed governing equation for the individual radionuclides can be employed also separately in a recursive implementation of the numerical solution of the ODE system. Finally, an integral balance strategy is employed to enhance convergence behavior. In this study we tested the accuracy of the solution against previous results by van Genuchten [29] and Lung et al. [30], who used analytical solutions derived for far more restrictive transport conditions.

The hybrid solution will be applied to four different scenarios for the migration of radioactive contaminants from liquid waste ponds at the Uranium mining facility of INB (Industrias Nucleares do Brasil) located near the municipality of Caetité, Bahia, Brazil. The solution procedure was selected because of its unique advantages for analysis of long-term contaminant transport problems (which for certain applications may run for tens of thousands of years), and because the approach is one of the recommended methods for radioactive waste safety assessment by the International Atomic Energy Agency [31, 32]. Calculated radionuclide concentrations are further used in subsequent radiation dose calculations. Safety or dose calculations for long time periods are essential for the management of long-lived radioactive wastes [3, 33]. Since institutional controls may not last much longer than a few

decades after site closure, the wastes are unlikely to remain safe. Natural leaching of radionuclides from the repository into the adjacent biosphere is almost certainly to occur within a few centuries or even earlier. Since mining wastes containing low-level natural radioactive materials are typically deposited in industrial landfills, regulations in Brazil and elsewhere require a safety assessment of the disposal facility using a leaching and off-site contaminant transport scenario.

Problem Formulation and Solution Methodology

Our conceptual model for the site involves a liquid waste pond, an underlying unsaturated soil zone through which water flows vertically downward, a permanently saturated granular aquifer through which water flows laterally, and a corresponding mixing zone where water from the unsaturated zone mixes with the saturated zone (Fig. 1). The recharge rate through the unsaturated zone into groundwater is defined by the long-term hydrologic characteristics of the site, thus disregarding operational conditions and the relatively short time period needed to fill the pond. Lateral flow through the aquifer is directly obtained from the hydraulic gradient and the saturated hydraulic conductivity. The mixing process of unsaturated recharge water and its dissolved constituents with water laterally moving through the saturated zone was modeled using the EPA mixing zone model [34] based on a penetration depth concept.

To solve the radionuclide transport problem with the hybrid method [16–18], one-dimensional transient advection–dispersion equations are assumed for each of the N_r species in the radionuclide decay chain. The solution procedure is first described for the saturated medium. The governing transport equations for the individual species are given by:
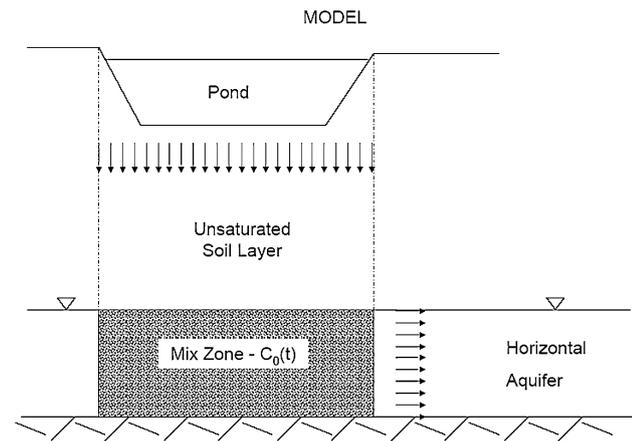
MODEL

Fig. 1 Schematic of the adopted conceptual model for vertical infiltration into residual unsaturated soil coupled to lateral flow in a horizontal granular aquifer

$$R_i \frac{\partial C_i}{\partial t} + V \frac{\partial C_i}{\partial x} = D \frac{\partial^2 C_i}{\partial x^2} - \mu_i R_i C_i(x,t) + \mu_{i-1} R_{i-1} C_{i-1}(x,t),$$
$$0 \le x \le L, \quad t > 0, \quad i = 1, \ldots, N_r \tag{1}$$

The associated initial and boundary conditions are

$$C_i(x,0) = 0, \quad 0 \le x \le L, \quad i = 1,..,N_r \tag{2}$$

$$-D \frac{\partial C_i}{\partial x} + V C_i = V f_i(t) \quad or \quad C_i = f_i(t), \quad x = 0, \quad t > 0,$$
$$i = 1, \ldots, N_r \tag{3}$$

$$-D \frac{\partial C_i}{\partial x} + h C_i = 0, \quad x = L, \quad t > 0, \quad i = 1, \ldots, N_r \tag{4}$$

where $f_i(t)$ is the concentration of the i-th radionuclide at the inlet. The boundary conditions at $x = 0$ can be of a third or first type, while the exit boundary condition can be of a third or second type depending upon the selected value for the mass transfer coefficient h. Before applying the Generalized Integral Transform Technique (GITT), an analytical filtering approach is used first to homogenize the boundary conditions at $x = 0$, which will improve convergence of the proposed eigenfunction expansions. While several filtering methods are available for this purpose [35, 36], here we use a very simple filter that employs the boundary source term concentration, as follows:

$$C_i(x,t) = C_i^*(x,t) + f_i(t), \quad 0 \le x \le L, \quad t > 0,$$
$$i = 1, \ldots, N_r \tag{5}$$

The transient advection–dispersion problem with homogeneous boundaries can now be rewritten in the form

$$R_i \frac{\partial C_i^*}{\partial t} + V \frac{\partial C_i^*}{\partial x} = D \frac{\partial^2 C_i^*}{\partial x^2} - \mu_i R_i C_i^* + \mu_{i-1} R_{i-1} C_{i-1}^* + g_i(t),$$
$$0 \le x \le L, \quad t > 0, \quad i = 1, \ldots, N_r \tag{6}$$

$$g_i(t) = -R_i \frac{df_i(t)}{dt} - \mu_i R_i f_i(t) + \mu_{i-1} R_{i-1} f_{i-1}(t), \quad t > 0,$$
$$i = 1, \ldots, N_r \tag{7}$$

$$C_i^*(x,0) = -f_i(0), \quad 0 \le x \le L, \quad i = 1, \ldots, N_r \tag{8}$$

$$-D \frac{\partial C_i^*}{\partial x} + V C_i^* = 0, \quad x = 0; \quad \frac{\partial C_i^*}{\partial x} = 0, \quad x = L,$$
$$t > 0, \quad i = 1, \ldots, N_r \tag{9}$$

To illustrate the remainder of the solution procedure, we use the above third type inlet and second type exit boundary conditions. The following auxiliary eigenvalue problem results:

$$D \frac{d^2 \varphi_n(x)}{dx^2} + \lambda_n^2 \varphi_n(x) = 0, \quad 0 < x < L \tag{10}$$

$$-D\frac{d\varphi_n(x)}{dx} + V\varphi_n(x) = 0, \quad x = 0; \quad \frac{d\varphi_n(x)}{dx} = 0, \quad x = L \tag{11}$$

This Sturm-Louiville problem is readily solved for the eigenfunctions and the related eigenvalues and norms:

$$\varphi_n(x) = \cos\left(\frac{\lambda_n}{\sqrt{D}}x\right) + \frac{V\sin\left(\frac{\lambda_n}{\sqrt{D}}x\right)}{\lambda_n\sqrt{D}} \tag{12}$$

$$\lambda_n \sin\left(\frac{\lambda_n}{\sqrt{D}}L\right) = \frac{V\cos\left(\frac{\lambda_n}{\sqrt{D}}L\right)}{\sqrt{D}} \tag{13}$$

$$norm_n = \int_0^L \varphi_n^2(x)dx = \frac{2V\lambda_n - 2V\lambda_n\cos\left(\frac{2\lambda_n}{\sqrt{D}}L\right) + \frac{(-V^2 + D\lambda_n^2)\sin\left(\frac{2\lambda_n}{\sqrt{D}}L\right)}{\sqrt{D}} + \frac{2L\lambda_n(V^2 + D\lambda_n^2)}{D}}{4\lambda_n^3} \tag{14}$$

The integral transform pair is defined next in terms of an eigenfunction expansion for the filtered concentrations, $C_i^*(x,t)$, by taking the eigenfunctions, $\varphi_n(x)$, as the basis for the expansions:

$$\bar{C}_{i,n}^*(t) = \int_0^L \varphi_n(x)C_i^*(x,t)dx \quad \rightarrow \quad Transform \tag{15}$$

$$C_i^*(x,t) = \sum_{n=1}^{\infty} \frac{\varphi_n(x)}{norm_n}\bar{C}_{i,n}^*(t) \quad \rightarrow \quad Inverse \tag{16}$$

By implementing the above filtered problem using $\int_0^L \varphi_n(x)dx$, the space variable x is eliminated, leading to the following transformed problem involving an infinite system of ordinary differential equations in time:

$$R_i\frac{d\bar{C}_{i,n}^*(t)}{dt} + V\sum_{m=1}^{\infty} a_{n,m}\bar{C}_{i,m}^*(t)$$
$$= -\lambda_n^2\bar{C}_{i,n}^*(t) - \mu_i R_i\bar{C}_{i,n}^*(t) + \mu_{i-1}R_{i-1}\bar{C}_{i-1,n}^*(t) + g_i(t)\bar{f}_n,$$
$$t > 0, \quad i = 1,\ldots,N_r, \quad n = 1,2,\ldots \tag{17}$$

where

$$a_{n,m} = \frac{1}{N_m}\int_0^L \varphi_n(x)\varphi_m'(x)dx \tag{18}$$

$$\bar{f}_n = \int_0^L \varphi_n(x)dx \tag{19}$$

and with the transformed initial conditions given by

$$\bar{C}_{i,n}^*(0) = -f_i(0)\bar{f}_n = -\frac{\left[V - V\cos(\frac{l_n}{\sqrt{D}}) + \sqrt{D}\sin(\frac{l_n}{\sqrt{D}})l_n\right]f_i(0)}{l_n^2} \tag{20}$$

The above transformed system, while amenable of analytical treatment using the corresponding coefficient matrix eigensystem analysis, is most flexibly handled using the *NDSolve* routine of *Mathematica 5.2* [26] to generalize the solution procedure to unsaturated systems as will be discussed later. Once the transformed concentrations are obtained numerically using *Mathematica*, an interpolating function is automatically generated to provide the time behavior in a continuous fashion. The inverse can then be recalled to explicitly provide the spatial dependency of the concentration fields.

For the more general situation of an unsaturated soil, the governing transport equations are given by

$$\frac{\partial[(\theta + \rho Kd_i)C_i]}{\partial t} + \frac{\partial(qC_i)}{\partial x} = \frac{\partial}{\partial x}(\theta D\frac{\partial C_i}{\partial x})$$
$$- \mu_i(\theta + \rho Kd_i)C_i(x,t) + \mu_{i-1}(\theta + \rho Kd_{i-1})C_{i-1}(x,t),$$
$$0 \le x \le L, \quad t > 0, \quad i = 1,\ldots,N_r \tag{21}$$

For long-term simulations such as those considered here (i.e., in the order of thousands of years), a time invariable recharge rate can be assumed, in which case the water content will be a function of position only. The formulation then simplifies to

$$[\theta(x) + \rho Kd_i]\frac{\partial C_i}{\partial t} + q\frac{\partial C_i}{\partial x} = \alpha q\frac{\partial^2 C_i}{\partial x^2} - \mu_i[\theta(x)$$
$$+ \rho Kd_i]C_i(x,t) + \mu_{i-1}[\theta(x) + \rho Kd_{i-1}]C_{i-1}(x,t),$$
$$0 \le x \le L, \quad t > 0, \quad i = 1,\ldots,N_r \tag{22}$$

where $\theta(x)$ is used to indicate that the water content is a function of the spatial coordinate, x. The corresponding initial and boundary conditions are

$$C_i(x,0) = 0, \quad 0 \le x \le L, \quad i = 1,\ldots,N_r \tag{23}$$

$$-\alpha \frac{\partial C_i}{\partial x} + C_i = f_i(t) \quad \text{or} \quad C_i = f_i(t), \quad x = 0, \quad t > 0,$$
$$i = 1, \ldots, N_r$$

(24)

$$-\alpha \frac{\partial C_i}{\partial x} + h^* C_i = 0, \quad x = L, \quad t > 0, \quad i = 1, \ldots, N_r$$

(25)

in which we used the definition of the dispersion coefficient as the product of the dispersivity, α, and the recharge pore-water velocity, V (i.e., $D = \alpha V$).

The integral transforms of the system of equations given by Eqs. (22) to (25) are very similar to those of the saturated medium, and as such will not be repeated here. The only difference is that the integral transformation in this case generates other coupling terms, including the coupling matrix for the transient terms of the transformed concentrations. For any arbitrary water content distribution, $\theta(x)$, we may adopt a semi-analytical integration procedure to generate the coefficient matrix with substantial savings in computational effort [37]. Also, the input profile for the water content depends on the solution of the nonlinear flow problem for the unsaturated zone as given by the Richards equation for steady-state flow. That initial profile was obtained with the HYDRUS-1D software package [38] based on a numerical solution of the Richards equation [39] for the soil profile being considered assuming a steady infiltration rate as dictated by the long-time recharge rate in the study area.

Numerical Verification

The above hybrid numerical-analytical procedure was implemented in the *Mathematica* 5.2 system [26], including all of the symbolic calculations of the solution process. The numerical accuracy of the resulting algorithm was tested against two codes previously developed for radionuclide decay chains: The LBL (Lawrence Berkeley Laboratory) computer code of Lung et al. [30] and the CHAIN code of van Genuchten [29]. Solutions employed in these codes were derived using Laplace transform techniques as applied to semi-infinite media.

Comparison with the Lawrence Berkeley Laboratory Code of Lung et al. [30]

The LBL code deals with purely advective transport (no dispersion) of radionuclides in saturated semi-infinite media to allow for explicit analytical inversion of the Laplace transforms. We consider here the three element LBL chain example formed by ^{234}U, ^{230}Th, and ^{226}Ra because of its similarity with the chain to be analyzed later for the Caetité

site. The following parameter values were used: $D = 50$ m^2/year, $\theta = 3 \times 10^{-3}$, $V = 1$ m/year, $R_1 = 120$, $R_2 = 1,500$, $R_3 = 300$, $\mu_1 = 2.806 \times 10^{-6}$ year^{-1}, $\mu_2 = 8.664 \times 10^{-6}$ year^{-1}, and $\mu_3 = 4.332 \times 10^{-4}$ year^{-1}. The normalized concentrations at boundary $x = 0$ are given by $f_1 = 1, f_2 = 1$, and $f_3 = 10$. Numerical results were obtained for the same time values (10 and 1,000 years) as used by Lung et al. (1987), while we used a domain length $L = 200$ m to avoid any effects of the exit boundary. Figure 2 compares calculated radionuclide concentration distributions for the two solutions at $t = 1,000$ years. Accounting for some loss in precision from directly reading the graphs in the LBL report [30], the agreement is very good. While the GITT results were obtained for system truncation orders $N < 150$, graphical convergence was attained much earlier. Figure 2 shows relatively rapid advancement of the contamination plumes for ^{234}U and ^{226}Ra, which have much lower retardation coefficients in comparison with ^{230}Th. Table 1 illustrates the convergence behavior of the eigenfunction expansion for ^{234}U at $t = 1,000$ years. The selected truncation orders were $N = 50, 75, 100, 125$ and 150 for the whole solution domain. Convergence is overall very satisfactory, yielding five or six significant digits in the results. The GITT solution hence was found to be precise in predicting concentrations that are orders-of-magnitude smaller than those at the inlet. This is important since utilities are usually required to satisfy environmental health criteria at the edge of their property, which in general involve much lower concentrations than at the source of contamination.

Comparison with the CHAIN Code of van Genuchten [29]

The CHAIN code considers the advective–dispersive transport of a radionuclide decay chain of up to four species. For the present test we employed the four element
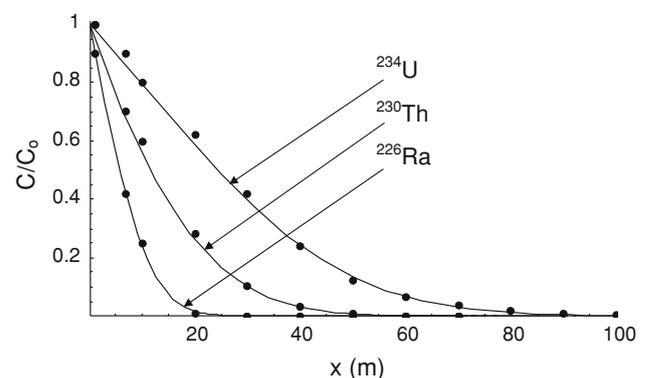
Fig. 2 Comparison of concentration distributions at $t = 1,000$ years for three radionuclides (^{234}U, ^{230}Th, and ^{226}Ra) as obtained in this study using GITT (*solid lines*) and by Lung et al. [30] using Laplace transforms (*symbols*)

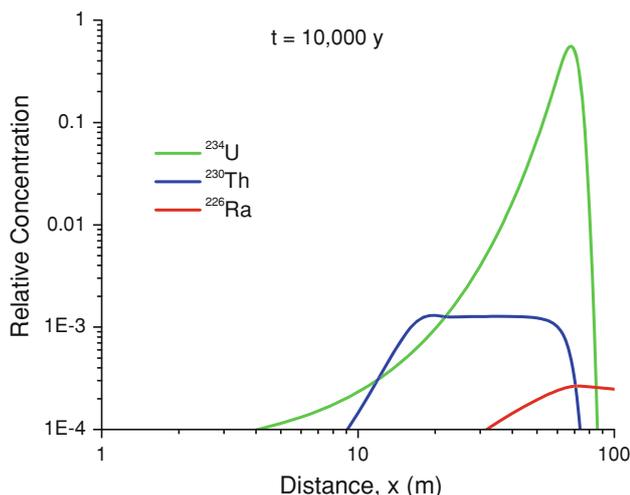**Table 1** Convergence of the GITT solution for ^{234}U concentration distribution at $t = 1,000$ years for the LBL test case of Lung et al. [30] involving ^{234}U, ^{230}Th and ^{226}Ra (N is the truncation limit)

x [m]	$N = 50$	$N = 75$	$N = 100$	$N = 125$	$N = 150$
1	0.980879	0.980935	0.980955	0.980962	0.980963
10	0.797314	0.797306	0.797301	0.797300	0.797300
20	0.585814	0.585807	0.585811	0.585810	0.585810
30	0.393687	0.393696	0.393693	0.393694	0.393694
40	0.240582	0.240578	0.240579	0.240579	0.240579
60	0.0663583	0.0663609	0.0663615	0.0663618	0.0663619
80	0.0119769	0.0119747	0.0119757	0.0119756	0.0119755
100	0.00139205	0.00139003	0.00139092	0.00139085	0.00139068

Table 2 Convergence of the GITT solution for the relatively concentration distribution of ^{264}Ra at $t = 10,000$ years for the test case of van Genuchten [29] involving ^{238}Pu, ^{234}U, ^{230}Th, and ^{226}Ra (N is the truncation order)

x [m]	$N = 50$	$N = 100$	$N = 150$	$N = 200$	$N = 250$	CHAIN
10	1.2737 E−6	1.5689 E−6	1.5630 E−6	1.5629 E−6	1.5663 E−6	1.5111 E−6
20	3.5447 E−5	3.5923 E−5	3.5927 E−5	3.5927 E−5	3.5934 E−5	3.5898 E−5
30	8.9891 E−5	9.0126 E−5	9.0136 E−5	9.0135 E−5	9.0138 E−5	9.0103 E−5
40	1.4340 E−4	1.4347 E−4	1.4346 E−4	1.4346 E−4	1.4346 E−4	1.4343 E−4
50	1.9501 E−4	1.9494 E−4	1.9494 E−4	1.9494 E−4	1.9494 E−4	1.9491 E−4
60	2.4041 E−4	2.4031 E−4	2.4031 E−4	2.4031 E−4	2.4031 E−4	2.4029 E−4
80	2.6106 E−4	2.6112 E−4	2.6112 E−4	2.6112 E−4	2.6112 E−4	2.6109 E−4
100	2.4736 E−4	2.4739 E−4	2.4739 E−4	2.4739 E−4	2.4739 E−4	2.4736 E−4

chain ^{238}Pu, ^{234}U, ^{230}Th, and ^{226}Ra as in [29] using inlet boundary conditions obtained from the exact solution of the Bateman equations for radioactive decay in and leaching from a waste site. We used the following parameter values: $D = 10$ m^2/year, $V = 100$ m/year, $R_1 = 10,000$, $R_2 = 14,000$, $R_3 = 50,000$, $R_4 = 500$, $\mu_1 = 7.9 \times 10^{-3}$ 1/year, $\mu_2 = 2.8 \times 10^{-6}$ 1/year, $\mu_3 = 8.7 \times 10^{-6}$ 1/year and $\mu_4 = 4.3 \times 10^{-4}$ 1/year. Numerical results were obtained at $t = 10,000$ years as provided also in [29],

while a domain length, L, of 300 m was sufficient to honor the semi-infinite medium assumption in our calculations. Table 2 illustrates the convergence behavior for ^{226}Ra for this strongly advective case. The various columns show GITT results for different truncation orders using increasing values of N. Also shown are the CHAIN results (last column) as obtained directly from the CHAIN software output.

The results in Table 2 indicate that the convergence rate of the eigenfunction expansions is again very good, yielding four digit agreement with the CHAIN benchmark solution, except near the inlet boundary. Figure 3 shows the concentrations of the four elements at $t = 10,000$ years. Notice that the ^{238}Pu concentrations are not visible within the invoked log concentration range, and that ^{226}Ra moves by far the fastest through the system because of its relatively low retardation factor.

Application to Uranium Waste Disposal Site

Our code using the GITT approach is now demonstrated for the environmental impact assessment of an industrial installation that deals with liquid and solid waste containing natural radioactive contaminants. The case study concerns possible pollution from an uranium mining and milling facility operated by INB (Indústrias Nucleares do Brasil) in Caetité (Bahia, Brazil). Liquid wastes resulting from the uranium extraction process were deposited in ponds within the mining installation. Each cell of the ponds

Fig. 3 Calculated concentration distributions versus distance for four radionuclides, ^{238}Pu, ^{234}U (*top curve*), ^{230}Th (*middle curve*), ^{226}Ra (*bottom curve*) at $t = 10,000$ years as obtained with GITT for the test case of van Genuchten [29]

Table 3 Scenarios considered for the migration of radionuclides from an uranium mining waste disposal pond

Case	Zones considered	L_1/L_2^{a} [m]	Infiltration[a]	Water content [m³/m³]	Kd's
1	Unsaturated/saturated	6.9/1,150	q = P − ET/Darcy	θ = 0.308/0.475	Table 4
2	Unsaturated/saturated	4.2/1,150	q = P − ET/Darcy	θ = 0.308/0.475	Table 4
3	Unsaturated/saturated	6.9/1,150	q = P/Darcy	θ = 0.338/0.475	Table 4
4	Unsaturated/saturated	6.9/1,150	q = P/Darcy	θ = 0.338/0.475	Clay[a]/Table 4

[a] L_1 = depth of unsaturated zone, L_2 = length of saturated zone, P = annual precipitation rate, ET = annual evapotranspiration rate, Darcy = flow rate estimated using Darcy's Law, Clay = Kd's of a clay soil

has an estimated operation period of 4 years. The Brazilian Nuclear Energy Commission (CNEN) required an analysis of the long-term transport of radioactive contaminants from the ponds into the subsurface, including an assessment of the total radioactive doses resulting from possible exposure to the radionuclides. Details of the analysis are given elsewhere [40], including model development, code construction, identification of flow and transport properties, and dose calculations. Here we focus on the contaminant transport simulations of four cases (Table 3) representing the most important possibilities for off-site migration.

The base case (Case 1) assumes a 6.9-m deep unsaturated zone below the pond, with recharge estimated from a hydrologic water balance of the Caetité region, and with water contents calculated with the HYDRUS-1D software package [38] using soil hydraulic properties [41] estimated from collected soil samples [40, 42]. The unsaturated zone was coupled to a horizontal granular aquifer of 1,150 m length. The flow rate through the horizontal aquifer was estimated from the hydraulic gradient and the hydraulic conductivity using Darcy's law.

The other three cases (2, 3, 4) considered here are relatively simple perturbations of the base case. Of these, Case 2 assumes a shallower unsaturated zone (4.2 m), typical of wet seasons in the area, while keeping the remaining parameters unchanged. Case 3 considers a much higher recharge rate through the unsaturated zone by considering only precipitation and neglecting evapotranspiration. Finally, Case 4 illustrates the importance of accurately estimating the partitioning coefficients, Kd's, of the radionuclides. In this case reported literature values for clay soils (stronger retardation) are used rather than the measured values listed in Table 4. Table 4 also gives estimates of the radioactive inventory of the simulated waste pond [40].

Calculated concentration distributions for the various cases are presented in Figs. 4 through 8. In each plot showing distributions versus distance, x, we employed black lines for ^{238}U and ^{234}U (graphs for these two radionuclides always coincided for the time periods considered

**Table 4** Partitioning coefficients, Kd [ml/g], and radioactive inventories, A [Bq]

Element	Kd [ml/g]	A [Bq]
^{238}U/^{234}U	2,985.6	5.34×10^{11}
^{230}Th	44,279.1	1.68×10^{10}
^{226}Ra	198.31	5.51×10^{10}
^{210}Pb	6,772.8	6.16×10^{11}

in this study), blue lines for ^{230}Th, red lines for ^{226}Ra, and green lines for ^{210}Pb.

Results for the base case (Case 1) were compared first with a very conservative scenario, not further referred to in Table 3, which completely neglects the unsaturated zone below the pond. Figure 4 show for this scenario the calculated concentration distributions along the horizontal aquifer after 500 years. Clearly, including the unsaturated zone considerably slows down the transport process, as expected, but also significantly lowers the maximum concentrations. These effects are most pronounced for lead, radium and thorium, which for our soils had much larger values of the retardation factors as compared to uranium.

Figures 5 shows for Case 1 the radionuclide concentration distributions in the aquifer at times $t = 1,000$, 2,000, 3,000, 4,000, and 10,000 years. Results again illustrate the relatively rapid migration of uranium (lower Kd values), but also very low concentrations characteristic of thorium transport. At the same time, radium and lead become more abundant at later times despite their relatively high retardation factors.

Figure 6 provides an interesting comparison between the base case and Case 2 (shallower unsaturated zone). The top plots show for the two cases concentration profiles of the radionuclides within the unsaturated zone at $t = 100$ years, while the plots at the bottom illustrate their migration along the horizontal aquifer at $t = 500$ years. Results again indicate that a thicker unsaturated zone (6.9 vs. 4.2 m) only minimally decreases the transport rate in the aquifer, but significantly reduces the maximum concentrations in the aquifer at similar total migration times.
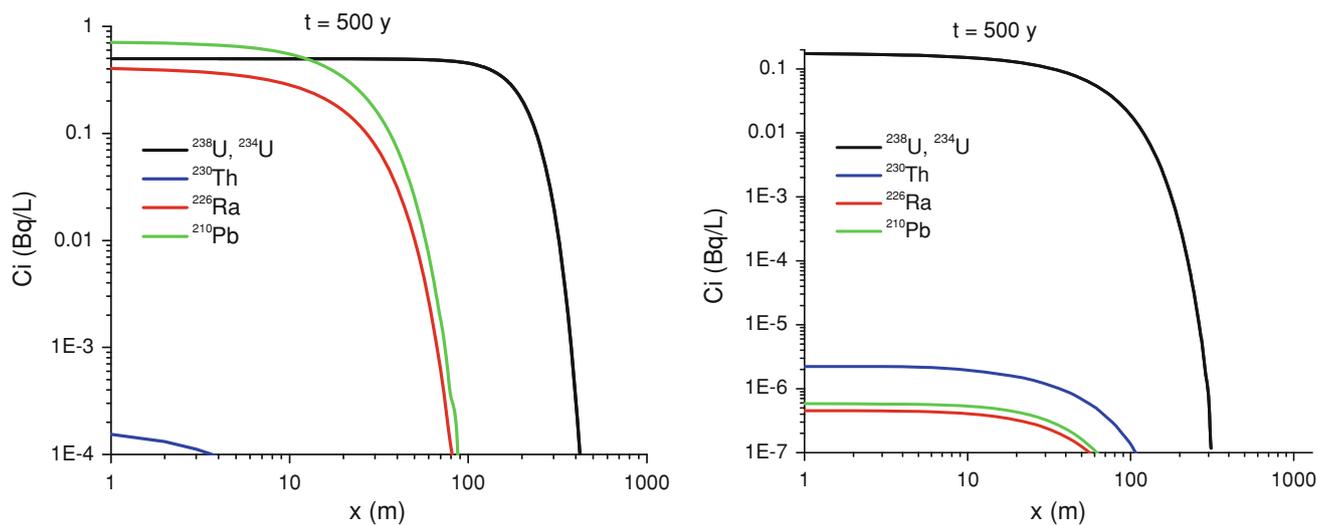
Fig. 4 Calculated radionuclide concentrations versus distance x in the horizontal aquifer for base Case without (*left*) and with (*right*) accounting for the unsaturated zone
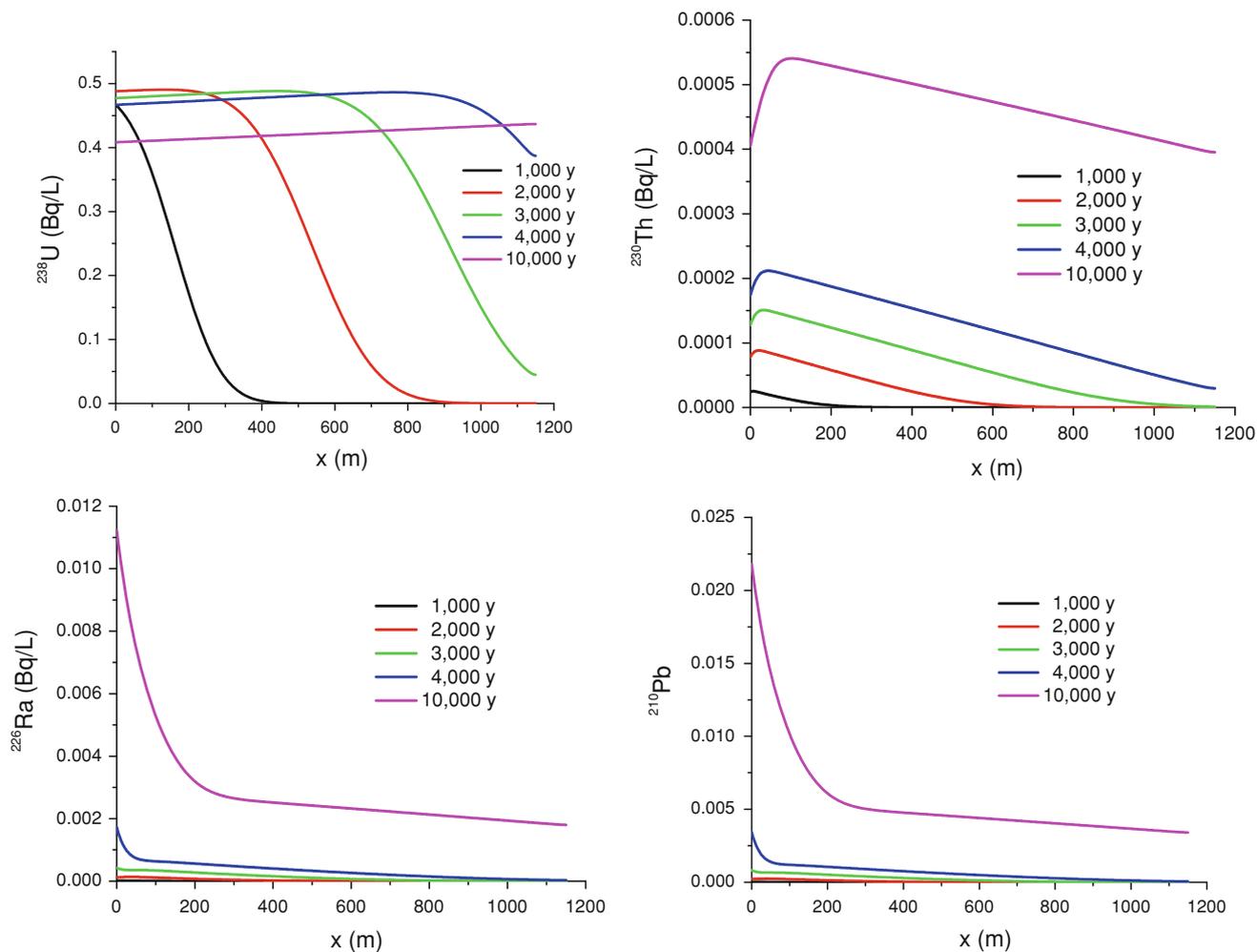
Fig. 5 Calculated radionuclide concentrations versus distance x in the horizontal aquifer for base Case 1 (with unsaturated zone). Shown are the distributions for ^{238}U (*top left*), ^{230}Th (*top right*), ^{226}Ra (*bottom left*) and ^{210}Pb (*bottom right*)
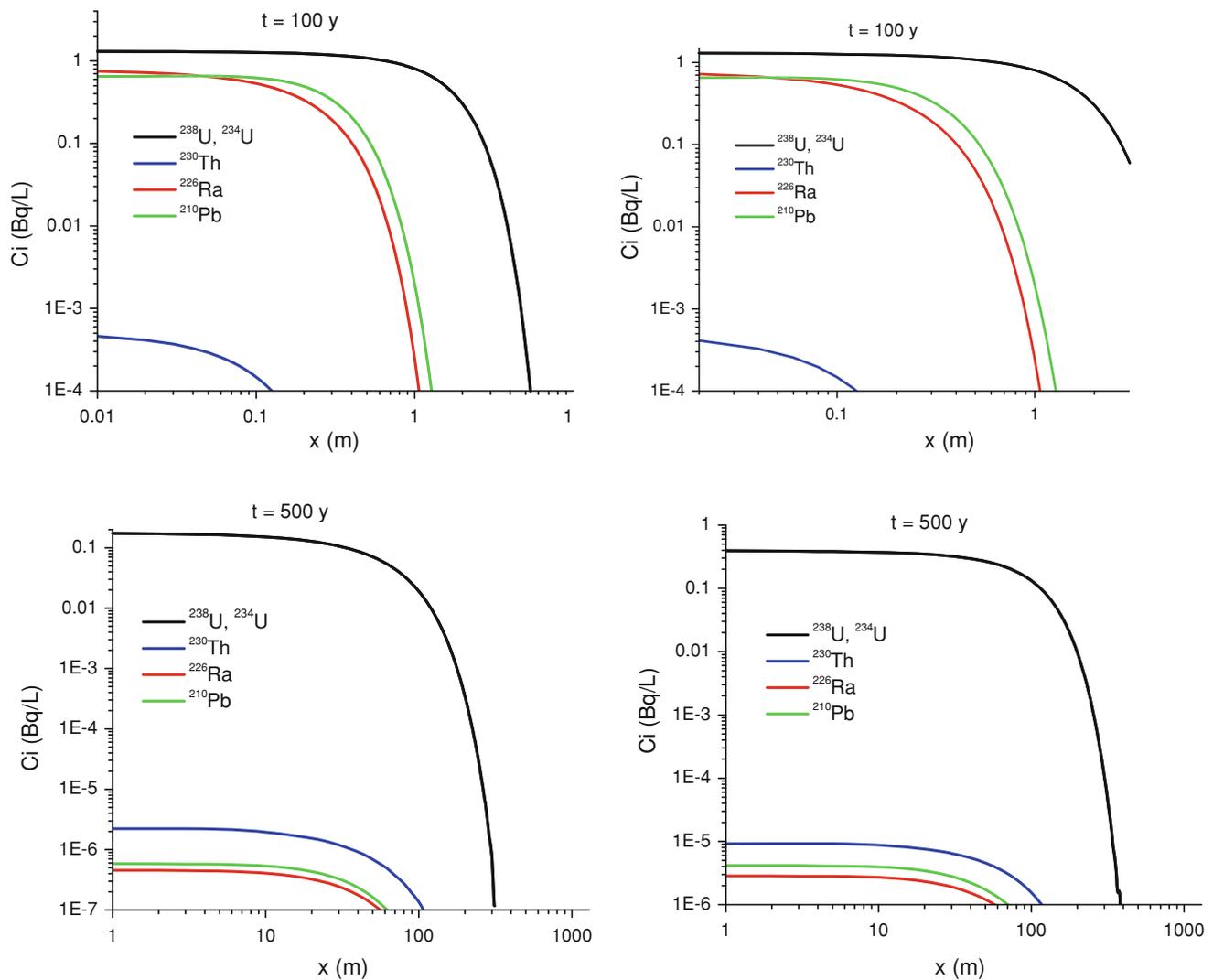
Fig. 6 Calculated radionuclide concentrations versus depth in the unsaturated zone (*top*) and the horizontal aquifer for base Case 1 (6.9 m deep vadose zone, *plots* on the *left*) and Case 2 (4.2 m vadose zone; *plots* on the *right*)

The effect of a higher recharge rate (Case 3; 1.104 m/year) relative to Case 1 (0.471 mm/year) is shown in Fig. 7. The top plots show concentrations in the unsaturated zone at $t = 500$ years, while the plots at the bottom show radionuclide transport in the aquifer at $t = 10,000$ years. The higher recharge rate for Case 3 (plots on the right) causes more rapid transport of the contaminants, which now move much further into to aquifer at similar elapsed times, and with higher concentrations.

Figure 8 next compares Case 1 (plots on the left side) with Case 4 for no evapotranspiration (higher recharge rate) and higher Kd values (plots on the right). The top plots present ^{238}U and ^{234}U concentrations in the unsaturated zone for times up to 1,000 years, while the bottom plots show the radionuclide distributions in the aquifer at $t = 500$ years. The higher Kd values typical of clay soils

lead to much higher retardation factors and hence to markedly different distributions for the two cases. For example, the U concentrations after 1,000 years in the unsaturated zone are much lower for Case 4 and, as expected, barely reach the horizontal aquifer after 500 years.

Performance Assessment

The main results of the performance and dose calculations are presented in this section. The primary objective of a performance or safety assessment is to provide evidence that the public and the environment are protected as much as possible in the future. This is possible by carrying out simulations and using the results to judge if the proposed
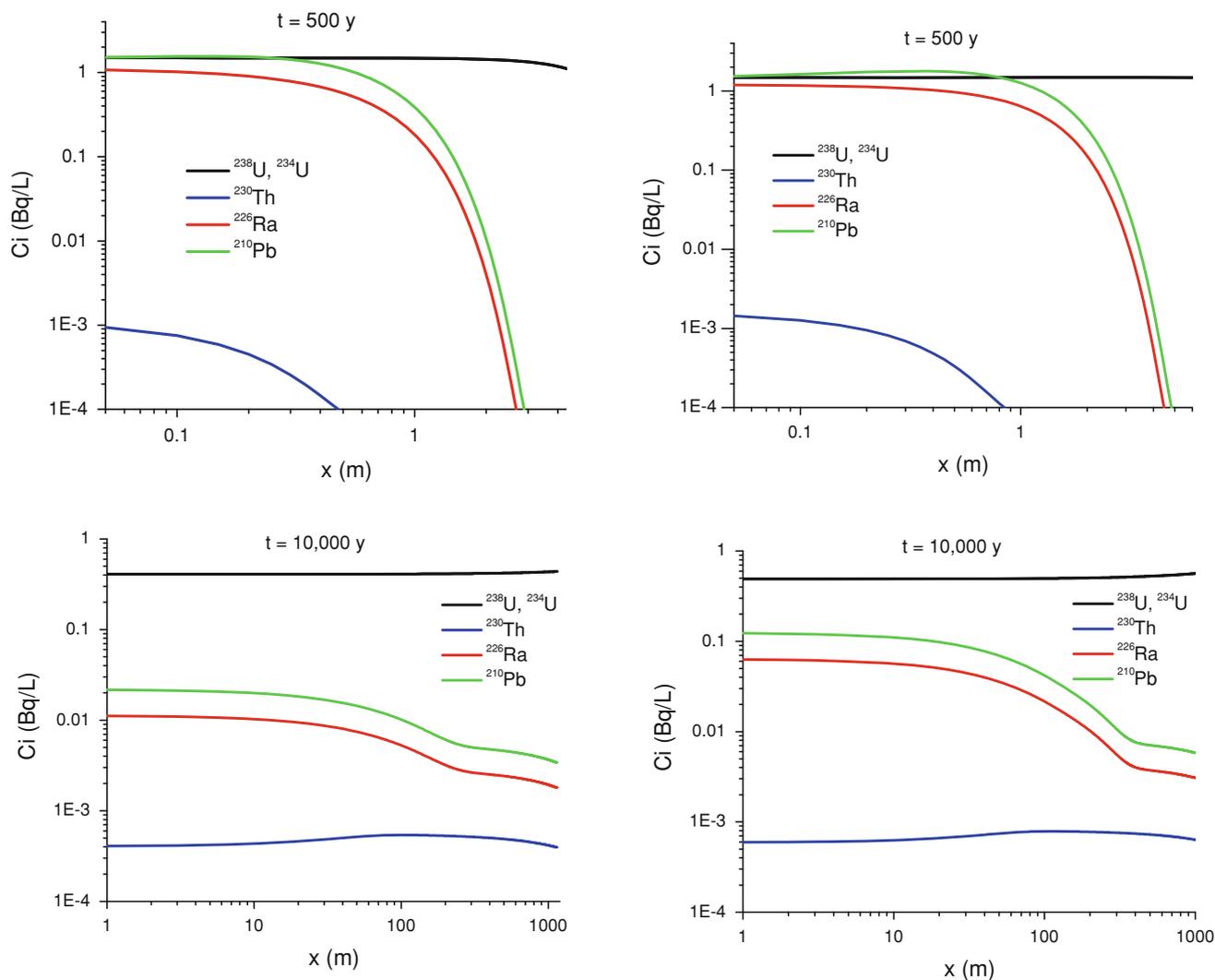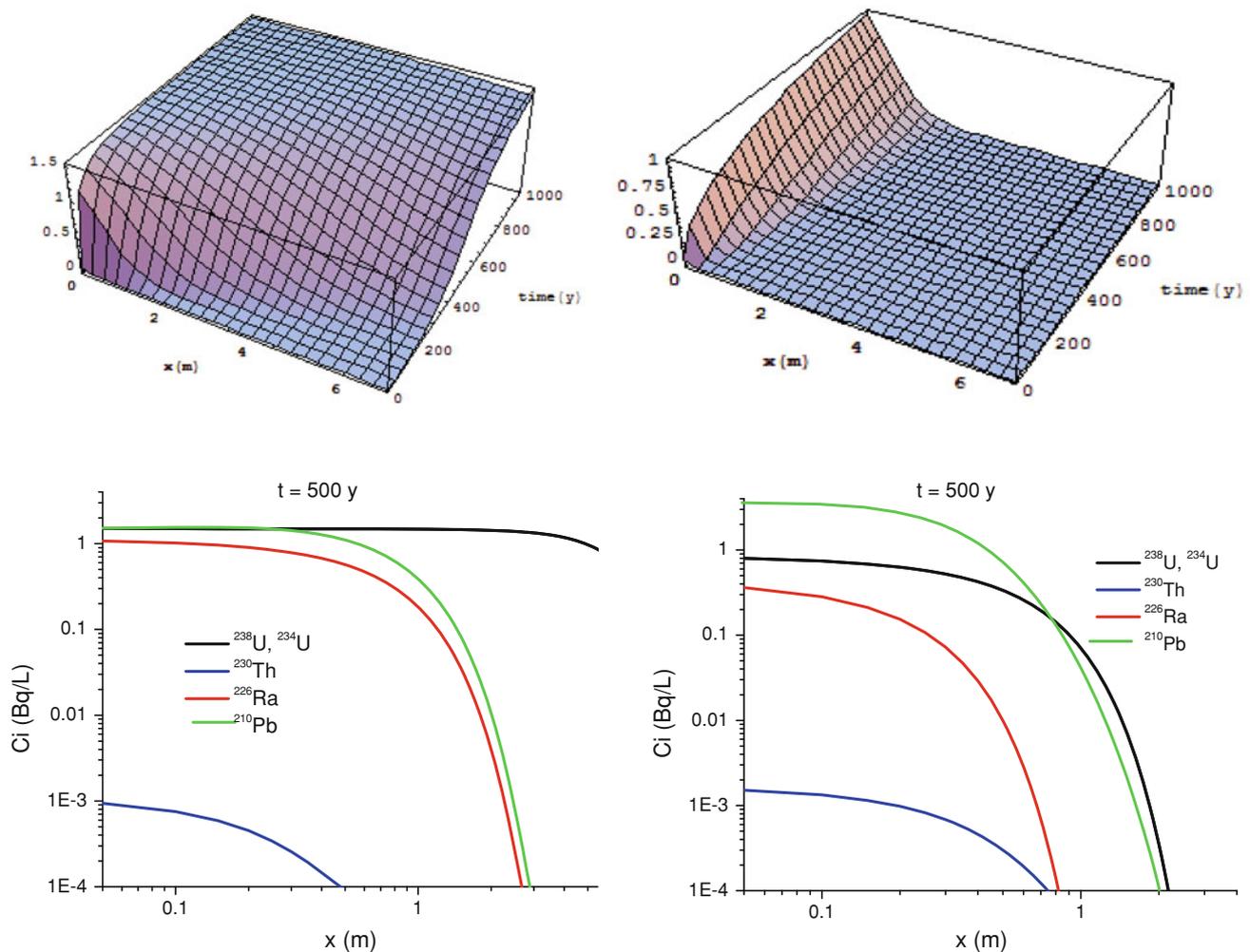
Fig. 7 Calculated radionuclide concentrations versus distance, x: in the unsaturated zone (*plots on top*) and horizontal aquifer (*bottom*) for Case1 having a low recharge rate (*left*) and Case 3 having a high recharge rate (*right*)

disposal site meets regulatory standards for long-term protection of human health and the environment. A pathway analysis with different scenarios permits a systematic way of evaluating potential routes by which the public could be exposed to radiation [6, 8, 43]. Because of the uncertain nature of the long-term integrity of disposal systems, as well as the unpredictability of human endeavors, all post-closure scenarios are by their very nature hypothetical.

The safety assessment assumes that the dose projection for members of the public cannot exceed 0.3 mSv/year above natural background. Assuming a risk factor of 5 % per Sievert (Sv) as recommended by ICRP [44], this leads to an assessed radiological risk of fatality to a potentially exposed group of 5×10^{-5} (i.e., 5 in one hundred thousand per year). The acceptable fraction, termed the dose or risk constraint, is generally determined by the regulatory

agency involved. For example, Brazilian regulations use a dose constraint of 0.3 mSv/y above natural background, which used in this study.

Consistent with calculations in the previous section, our performance assessment considered vertical flow through the waste site (pond) and the 6.9-m deep unsaturated zone, and subsequently horizontal flow through the underlying aquifer until water was intercepted by a well or discharged to a stream outside the URA. We assumed that the well or stream at that location was the only source of water for local residents for human consumption, irrigation or for use by farm animals. The radiological dose was calculated for an exposed critical group of individuals receiving the highest dose or risk. Data regarding human behavior were based on the dietary habits of adults from that group (e.g., water and food consumption, breathing rate, and number of hours being indoor or outdoor). Residents received doses

Fig. 8 Calculated ^{238}U radionuclide concentrations (Bq/L) versus depth, x, and time, t (*top plots*) and versus depth at $t = 500$ y (*bottom*) in the unsaturated zone for Case 1 (*left plots*) and Case 4 having a higher recharge rate and higher Kd values (*right*)

from external radiation, ingestion of contaminated water and food, and inhalation of airborne radionuclides transported from the waste site or suspended in runoff water following irrigation. Following previous studies [6, 32], the following 10 specific processes in the biosphere were considered: (a) ingestion of water from the well, (b) irrigation, (c) re-suspension or particulates and inhalation, (d) external radiation exposure, (e) consumption of home-grown produce, (f) consumption of contaminated meat, (g) ingestion of contaminated milk, (h) accidental ingestion of contaminated soil, (i) inhalation of radon and decay products from soil, and (j) contact with surface water, including transfer to humans. However, we did consider the eating habits and current agricultural activities of the critical group for the dose calculations. For this reason we did not include exposure through the ingestion of fish since the local population has an abundant supply of fish from outside the region. The dose calculations also assumed current percentages of the local versus outside production of milk

and meat. The diet of the critical group was assumed to be based on manioc, rice, beans, potatoes and meat (both chicken and beef), while their fruits consisted of banana, orange and lemon, and their vegetable of carrot, bitter melon (chuchu), beet and some lettuce. Ingestion, inhalation and external dose conversion factors (Sv Bq^{-1}), as well as transfer coefficients and concentration factors were taken from IAEA [43].

We considered four scenarios: a Leaching Scenario (CEN1), a Human Intrusion Scenario (CEN2), a Farmer-Dweller Intrusion Scenario (CEN3) and a Road Builder Scenario (CEN4). Radionuclide concentrations calculated in the previous section were used for both the dose calculations of Leaching Scenario CEN1. The dose calculations presented here were carried out using methodologies developed by IAEA [43] as implemented by Pontedeiro [3].

For Leaching Scenario CEN1 we assumed that radionuclides migrated through an 1,850 m long horizontal
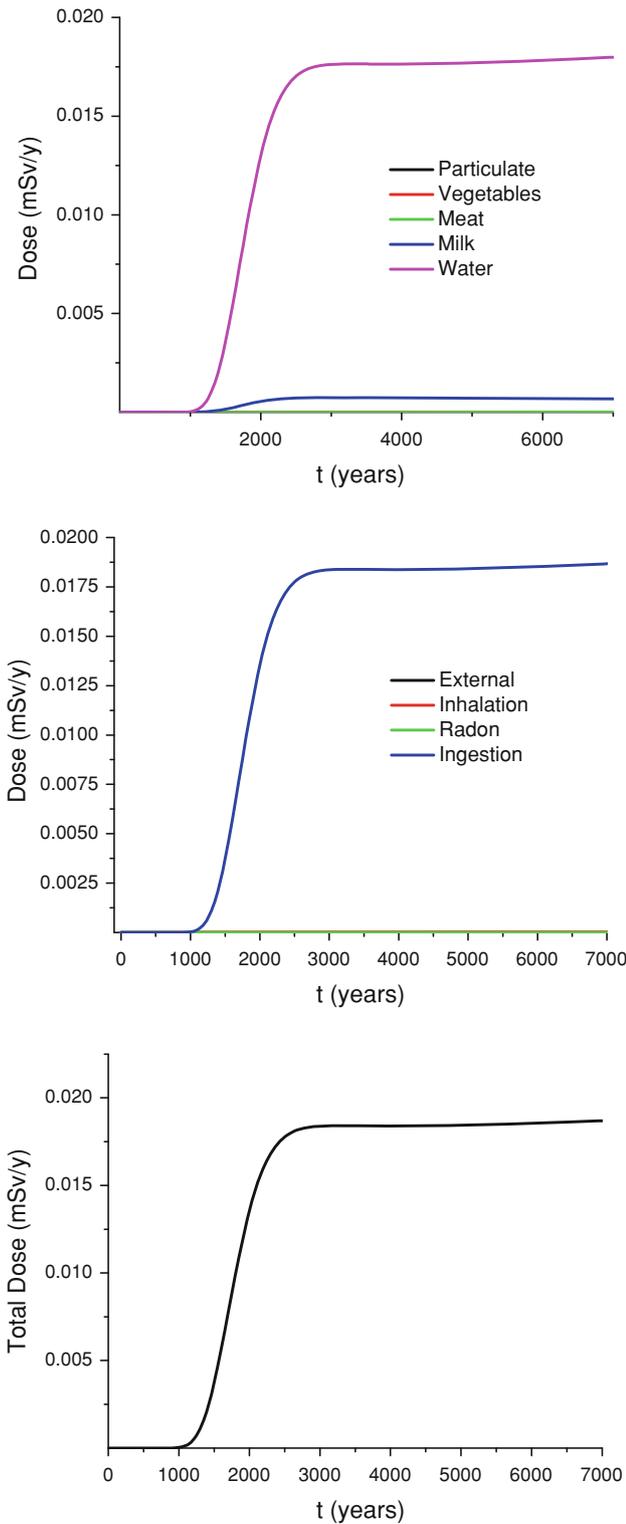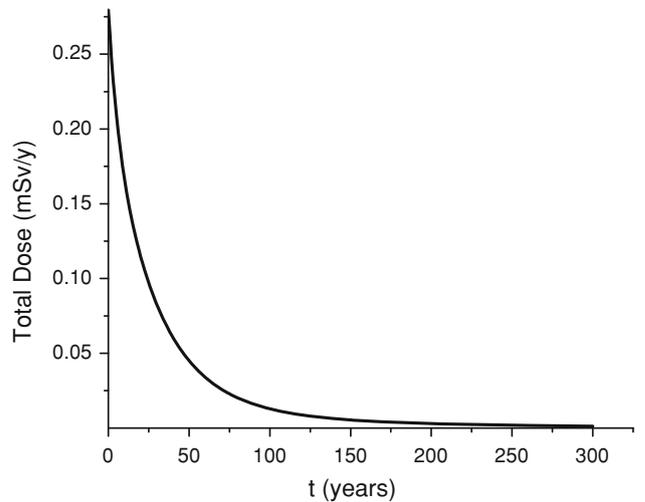
Fig. 9 Dose calculations for Leaching Scenario CEN1: Ingestion by different paths (*top*), exposure to different pathways (*middle*) and total dose (*bottom*)
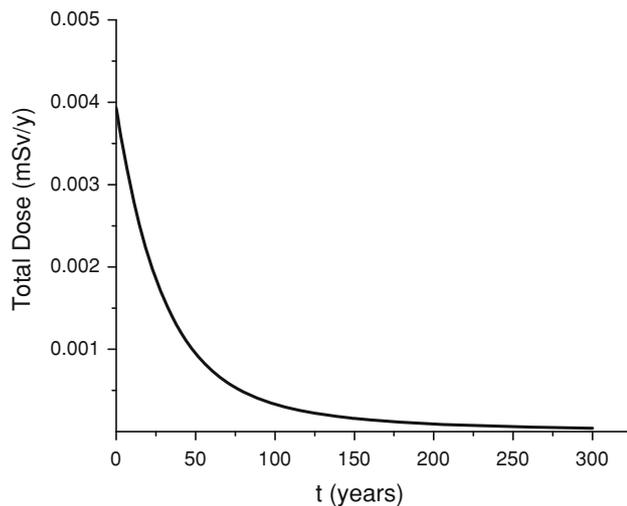
aquifer until reaching a small stream or well outside the URA boundary. Contaminated water was then used for irrigation and consumption by cattle and the farmer and his
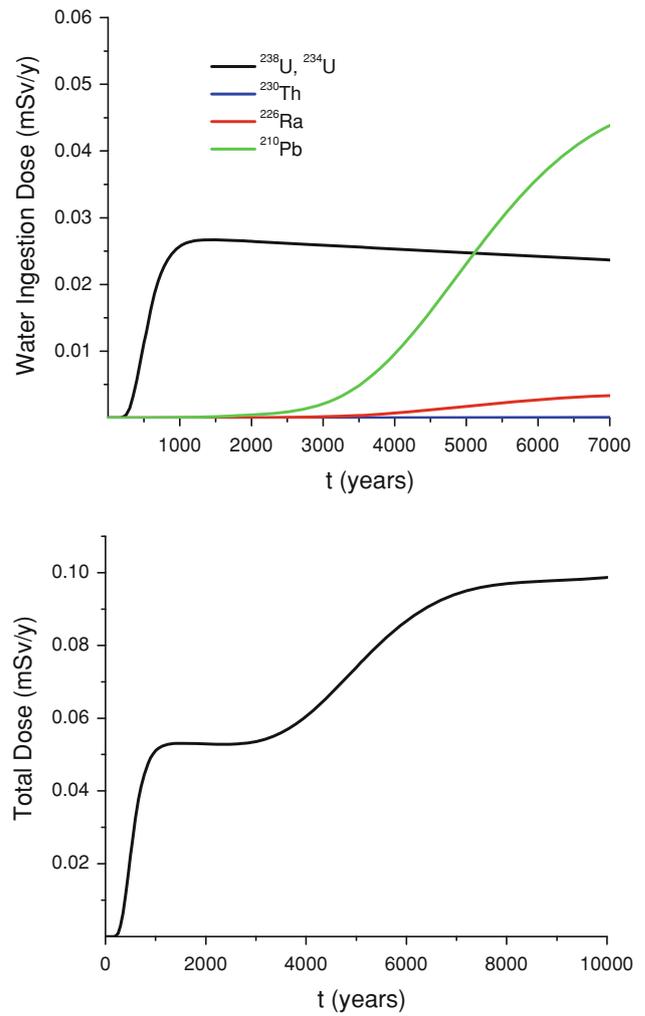
Fig. 10 Dose calculations for Human Intrusion Scenario CEN2: Doses due to ingestion of contaminated water (*top*) and total dose (*bottom*)

Fig. 11 Total dose for Farmer-Dweller Scenario CEN3

Fig. 12 Total dose for Road Builder Scenario CEN4

family. Dose calculations for CEN1 are presented in Fig. 9. Results indicate that the dose due to the ingestion of water was dominant as compared to the doses resulting from the other exposure pathways. The maximum total dose remained less than 0.0185 mSv/year during the first 10,000 years after closure of the repository. This maximum is far less than the Brazilian regulatory limit of 0.3 mSv/year above natural background. It is important to note that the total dose of the Leaching Scenario was almost zero for the first several thousands of years, being only 1.14×10^{-7} mSv/year at $t = 2,000$ years.

For the dose calculations of the Human Intrusion Scenario (CEN2), shown in Fig. 10, we used calculated radionuclide concentrations leaving the unsaturated zone below the original waste layer at a depth of 6.9 m. We assumed that intrusion occurred in the URA restricted area after institutional control ended, and that water was removed from the aquifer exactly under the embankment for ingestion. This water for ingestion was the only exposure pathway considered for CEN2. Doses of the five radionuclides resulting from this ingestion are presented in the top plot of Fig. 10. Notice that the ^{238}U and ^{234}U peaks occurred at about 1,000 years, while the dose due to Pb-210 increased during the entire 10,000 years considered here. The total dose of the Human Intrusion Scenario is shown in the bottom plot. The plot indicates a first peak due to ^{238}U and ^{234}U leaching, followed by increases later due to ^{210}Pb. The total dose value was 0.1007 mSv/year at 10,000 years, again below the Brazilian regulatory limit of 0.3 mSv/year above natural background.

For the Farmer-Dweller Intrusion Scenario (CEN3) we considered the presence in the area of a small rural settlement. The scenario assumes some dilution of the radioactive waste with nonradioactive materials (local soil). For the calculations we assumed that 10 % of the

waste was brought to the surface, and that the average specific activity of all material used by the residents was equal to the total activity of the waste divided by the total mass of the material used. For this scenario we included the 10 exposure pathways [7] listed earlier, except any ingestion of water by a well and exposure to surface water, including transfer to fish and humans. Figure 11 shows that the total dose for the CEN3 Framer-Dweller Scenario declined rapidly from a relatively high initial value of 0.28 mSv/year to very small values later.

Finally, for the Road Builders Scenario (CEN4) we considered inadvertent intrusion, and access to or removal of waste at or near the surface. The contaminated soil presumably was used for the construction of a road through the property. The road was assumed to be constructed at an average speed of 20 km per year, with the workers being present 8 h per day, 20 days per month. The contaminated material itself was assumed to be spread along a path equivalent to 1 km, with the road builders working with the contaminated material for a total of 90 h per year working. Expose pathways involved (a) external exposure to contaminated soil, (b) dust inhalation, and (c) accidental ingestion of contaminated soil. As shown in Fig. 12, the initial value of the total dose was calculated to be 0.004 mSv/year. This is far below the 0.3 mSv/year Brazilian regulatory limit. The total dose again declined very quickly with time, similarly as for scenario CEN3.

Concluding Remarks

Our results illustrate the considerable power of hybrid numerical-analytical solutions for evaluating relatively complex subsurface contaminant transport problems, in this case the long-term transport of radioactive contaminant decay chains in a coupled saturated and unsaturated soil-aquifer system, followed in this example by a risk assessment study. The generalized integral transform technique (GITT) produced analytical expressions for the concentration distributions versus distance, and analytical or numerical estimates of the concentration as a function of time. Especially attractive features of the hybrid method for long-time environmental assessment studies are its user-controlled accuracy and very efficient computational performance for non-transformable problems such as nonlinear water flow and contaminant transport formulations. Also, the ability to accurately solve the equations for very small concentrations (compared to the initial concentration) is an important attribute of the GITT method. In addition to straightforward error control and estimation, an attractive aspect of the method is its easy extension to multi-dimensional situations. This is due to the hybrid nature of the solution process since the analytical part is

employed for all but one independent variable, while the numerical part is used only for integration of a system of ordinary differential equations in one single independent variable, usually the time variable. As such, the approach can be extended in a relatively straightforward manner also to non-ideal transport processes such as contaminant transport in structured (fractured or macroporous) media [18], with concomitant problems of preferential flow. We finally note that the GITT approach is able to solve serial reactions in which the sequential reaction rate is equal to the previous reaction rate, which is a limiting feature that plagues most or all fully analytical solutions for sequential decay chain reactions [45]. In fact, since the reaction terms are not here included in the auxiliary eigenvalue problems, such singularities are not carried into the analytical portion of the solution, while the numerical solution of the transformed equations proceeds as normal. We conclude that the methodology followed in this paper is well suited for simulations of a broad range of especially long-term contaminant transport problems in soils and groundwater.

References

1. CNEN: Licensing of Radioactive Installations, Report No. CNEN-NE-6.02, Brazilian Nuclear Energy Commission, CNEN, Rio de Janeiro, Brazil (1998)
2. IAEA: Extent of environmental contamination by naturally occurring radioactive material (NORM) and technological options for mitigation, Technical Report Series No. 419, Int. Atomic Energy Agency (IAEA), Vienna (2003) (available at http://www-pub.iaea.org/MTCD/publications/Pubdetails.asp?pubId=6789)
3. Pontedeiro, E.M.: Avaliação de Modelos de Impacto Ambiental para Deposição de Resíduos Sólidos Contendo Radionuclídeos Naturais em Instalações Minero-Industriais, DSc Thesis, PEM/COPPE/UFRJ, Brazil (2006)
4. Heilbron, P.F.L., Perez-Guerrero, J.S., Pontedeiro, E.M., Ruperti Jr., N., Cotta, R.M.: Analytical model for environmental impact due to solid waste disposal from electricity generation. Hybrid Meth. Eng. **4**(1–2), 1–26 (2002)
5. Landa, E.R.: Naturally occurring radionuclides from industrial sources: characteristics and fate in the environment. Radioact. Environ. **10**, 211–237 (2007)
6. Pontedeiro, E.M., Heilbron, P.F.L., Cotta, R.M.: Assessment of mineral industry NORM/TENORM disposal in hazardous landfills. J. Hazard. Mater. **139**, 563–568 (2007)
7. Kennedy, J.D., Strenge, D.L.: Residual radioactive contamination from decommissioning: technical basis for translating contamination levels to annual total effective dose equivalent. NUREG CR-5512, PNL-7994, U.S. Nuclear Regulatory Commission, Washington, DC (1992)
8. Yu, C., Gnanapragasam, E., Zielen, Biwer, B,M., Kamboi, S., Cheng, J.-J., Yuan, Klett, T., LePoire, D., Ziele, A.J., Chen, S.Y., Williams, W.A., Wallo, A., Domotor, S., Mo, T., Schwartzman, A.: User's manual for RESRAD-OFFSITE, Version 2. ANL/EVS/TM/07-1, Argonne National Laboratory, Argonne, IL (2007)
9. Simunek, J., van Genuchten, M.T., Sejna, M.: Development and applications of the HYDRUS and STANMOD software packages and related codes. Vadose Zone J. **7**(2), 587–600 (2008)
10. Finsterle, S., Doughty, C., Kowalsky, M.B., Moridis, M.B., Pan, L., Xu, T., Zhang, Y., Pruess, K.: Advanced vadose zone simulations using TOUGH. Vadose Zone J. **7**(2), 601–609
11. Javandel, I., Doughty, C., Tsang, C.-F.: Groundwater Transport: Handbook of Mathematical Models. Water Resour. Monograph **10**, Am. Geophys. Union, Washington, D.C. (1984)
12. Leij, F.J., Skaggs, T.H., van Genuchten, M.T.: Analytical solutions for solute transport in three-dimensional semi-infinite porous media. Water Resour. Res. **27**(10), 2719–2733 (1991)
13. Bauer, P., Attinger, S., Kinzelbach, W.: Transport of a decay chain in homogenous porous media: analytical solutions. J. Contam. Hydrol. **49**, 217–239 (2001)
14. Vanderborght, J., Kasteel, R., Vereecken, H.: Stochastic continuum transport equations for field-scale solute transport: Overview of theoretical and experimental results. Vadose Zone J. **5**, 184–203 (2006)
15. Pérez Guerrero, J.S., Pimentel, L.C.G., Skaggs, T.H., Van Genuchten, M.T.: Analytical solution of the advection-diffusion transport equation using a change-of-variable and integral transform technique. Int. J. Heat Mass Transfer **52**, 3297–3304 (2009)
16. Cotta, R.M.: Integral Transforms in Computational Heat and Fluid Flow. CRC Press, Boca Raton (1993)
17. Cotta, R.M., Mikhailov, M.D.: Hybrid methods and symbolic computations. In: Minkowycz, W.J., Sparrow, E.M., Murthy, J.Y. (eds.) Handbook of Numerical Heat Transfer, 2nd edition, Chapter 16. Wiley, New York (2006)
18. Cotta, R.M., Ungs, M.J., Mikhailov, M.D.: Contaminant transport in finite fractured porous medium: integral transforms and lumped-differential formulations. Ann. Nucl. Energy **30**, 261–285 (2003)
19. Cotta, R.M., Mikhailov, M.D., Ruperti Jr., N.J.: Analysis of radioactive waste contamination in soils: solution via symbolic manipulation, Proceedings of the International Conference on the Radiological Accident of Goiânia; 10 Years Later, Brazil, October 1997 (CD-ROM); also in IAEA Conf. Proceedings Series, Vienna, IAEA-GOCP, pp. 298–308 (1998)
20. Liu, C., Szecsody, J.E., Zachara, J.M., Ball, W.P.: Use of the generalized integral transform method for solving equations of solute transport in porous media. Adv. Water Resour. **23**, 483–492 (2000)
21. Leal, M.A., Ruperti Jr, N.J.: A hybrid solution for simulation of 2-D contaminant transport in heterogeneous subsurface systems. Hybrid Methods Eng. **3**(2), 111–129 (2001)
22. Barros, F.P.J., Mills, W.B., Cotta, R.M.: Integral transform solution of two-dimensional model for contaminants dispersion in rivers and channels with spatially variable coefficients. Environ. Model. Softw. **21**, 699–709 (2006)
23. Skaggs, T.H., Jarvis, N.J., Pontedeiro, E.M., van Genuchten, M.T., Cotta, R.M.: Analytical advection-dispersion model for transport and plant uptake of contaminants in the root zone. Vadose Zone J. **6**, 890–898 (2007)
24. Pérez Guerrero, J.S., Skaggs, T.H., van Genuchten, M.T.: Analytical solution for multi-species contaminant transport in finite media with time-varying boundary conditions. Transp. Porous Media **85**, 171–188 (2010)
25. Cotta, R.M., Quaresma, J.N.N., Sphaier, L.A., Naveira-Cotta, C.P.: Unified integral transform approach in the hybrid solution of multidimensional nonlinear convection-diffusion problems. 14th Int. Heat Transfer Conf., Washington, DC, USA, August 2010
26. Wolfram, S.: Mathematica 5.2, Cambridge, UK, Wolfram Media (2005)
27. Bateman, H.: The solution of a system of differential equations occurring in the theory of radioactive transformations. Proc. Cambridge Philos. Soc. **15**, 423–427 (1910)
28. Higashi, K., Pigford, T.H.: Analytical models for migration of radionuclides in geologic sorbing media. J. Nucl. Sci. Technol. **17**(9), 700–709 (1980)

29. van Genuchten, M.T.: Convective-dispersive transport of solutes involved in sequential first-order decay reactions. Comput. Geosci. **11**(2), 129–147 (1985)

30. Lung, H.C., Chambré, P.L., Pigford, T.H., Lee, W.W.L.: Transport of radioactive decay chains in finite and semi-infinite porous media, Earth Sciences Division, Lawrence Berkeley Laboratory, Report LBL23987 (1987)

31. IAEA: Safety Assessment Methodologies for Near Surface Disposal Facilities, Vol. 1, Review and Enhancement of Safety Assessment Approaches and Tools, International Atomic Energy Commission (IAEA), Vienna, Austria (2004)

32. Heilbron, P.F.L., Xavier, A.M., Pontedeiro, E.M., Ferreira, R.S.: Segurança Nuclear e Proteção do Meio Ambiente. Brazil, Editora E-Papers, Rio de Janeiro (2004)

33. Pontedeiro, E.M., van Genuchten, M.T., Cotta, R.M., Simunek, J.: The effects of preferential flow and soil texture on risk assessments of a NORM waste disposal site. J. Hazard. Mater. **174**(1–3), 648–655 (2010)

34. EPA: Soil Screening Guidance: Technical Background Document, EPA/540/R-95/128, PB96–963502. Office of Solid Waste and Emergency Response, U.S. Environmental Protection Agency, Washington, DC (1996)

35. Almeida, A.R., Cotta, R.M.: A comparison of convergence acceleration schemes for eigenfunction expansions of partial differential equations. Int. J. Numer. Method. Heat Fluid Flow **6**(no. 6), 85–97 (1996)

36. Cotta, R.M., Mikhailov, M.D.: Heat Conduction: Lumped Analysis, Integral Transforms, Symbolic Computation. Wiley, New York (1997)

37. Sphaier, L.A., Cotta, R.M., Naveira-Cotta, C.P., Quaresma, J.N.N.: The UNIT algorithm for solving one-dimensional convection-diffusion problems via integral transforms. Int. Commun. Heat Mass Transf. **38**(5), 565–571 (2011)

38. Simunek, J., van Genuchten, M.T., Sejna, M.: The HYDRUS-1D Software Package for Simulating the One-Dimensional Movement of Water, Heat And Multiple Solutes in Variably-Saturated Media, Version 3.0. HYDRUS Software Series 1, Department of Environmental Sciences, University of California, Riverside, 240 p (2005)

39. Richards, L.A.: Capillary conduction of fluid through porous mediums. Physics **1**, 318–333 (1931)

40. Orlande, H.R.B., Cotta, R.M., Su, J., Couto, P., Naveira, C.P., Moreira, P.H.S., Sabino, V.: Estudo da Dispersão de Rejeitos Radioativos das Células dos Depósitos de Rejeitos Líquidos Tratados (Ponds) na Unidade de Concentrado de Urânio na INB-Caetité, BA, Relatório final COPPETEC Projeto PEM 7552 (2006)

41. van Genuchten, M.T.: A closed-form equation for predicting the hydraulic conductivity of unsaturated soils. Soil Sci. Soc. Am. J. **44**, 892–898 (1980)

42. Orlande, H.R.B., van Genuchten, M. T., Cotta, R.M., Moreira, P.H.: Bayesian estimation of hydraulic and solute transport parameters from laboratory soil columns experiments. In: Rebay, M. (ed.), Proc. Int. Symp. on Convective Heat and Mass Transfer in Sustainable Energy, CONV-09, April 26–May 1, Hammamet, Tunisia (2009)

43. IAEA: Safety assessment methodologies for near surface disposal facilities, Vol. 2, Test cases, Int. Atomic Energy Commission (IAEA), Vienna, Austria (2004)

44. ICRP: Radionuclide Transformations Energy and Intensity of Emissions. International Commission on Radiological Protection, ICRP Publ. 38. Pergamon Press, Oxford (1983)

45. Sun, Y., Petersen, J.N., Clement, T.P., Skeen, R.S.: Development of analytical solutions for multispecies transport with serial and parallel reactions. Water Resour. Res. **35**(1), 185–190 (1999)